



# Improvement of Overlap for 2×2 MZI Electro-Optic Switch Based on Lithium Tantalite (LiTaO<sub>3</sub>)

Sadeq A. Hbeeb

## **Authors affiliations:**

Department of  
Communications, University of  
Diyala, Diyala - Iraq.  
[Sadeq.hbeeb@gmail.com](mailto:Sadeq.hbeeb@gmail.com)

## **Paper History:**

**Received:** 17<sup>nd</sup> Mar. 2022

**Revised:** 9<sup>th</sup> May 2022

**Accepted:** 31<sup>st</sup> May 2022

## **Abstract**

This research introduces a method of an electro-optic effect and electro-refractive effect that considers very imperative for high-speed optical communication systems. In this research, it presents way by a reduction the gap between the electrodes  $d$ , and this technique achieves to solve the problem of overlap for Mach-Zehnder interferometer MZI electro-optical switch base on lithium tantalite LiTaO<sub>3</sub>, also this technique suggests a model for analysis the effect parameters on the electro-optic overlap of the electro-optic switch as the ordinary positive changing of refractive index and a length of arm switch. This study achieves a better overlap by large positive changing refractive index with a suitable small length of arm about  $8\mu\text{m}$  and low driving power at least  $4\text{V}/\mu\text{m}$ . Also, for lithium tantalite LiTaO<sub>3</sub>, this research achieves a better performance for system using the near infrared wavelength.

**Keywords:** Mach-Zehnder Interferometer (MZI), Electro-Optic Switch, Electro-Optic Effect, Electro- Refractive Effect, Lithium Tantalite LiTaO<sub>3</sub>.

تحسين التشابك للمفتاح (2\*2MZI) الكهروضوئي المستند على الليثيوم تننليات  
LiTaO<sub>3</sub>

صادق عدنان حبيب

## **الخلاصة:**

البحث يقدم طريقة التأثير الكهروضوئي وطريقة الانكسار الألكتروني التي تعتبر مهمة جدا في انظمة الاتصالات الضوئية العالية السرعة. في هذا البحث يقدم طريقة لحل مشكلة التشابك للمفتاح الكهروضوئي نوع ماج زيندر (MZI) المكون من مادة الليثيوم تننليات LiTaO<sub>3</sub> بواسطة اقتراح تقنية تخفيض الفجوة بين الأقطاب  $d$ . كذلك في هذه التقنية اقتراح نموذج رياضي لتحليل العوامل المؤثرة على التشابك الكهروضوئي مثلا "التغير الايجابي لمعامل الانكسار و طول الذراع للمفتاح الكهروضوئي". في هذا البحث تم انجاز تشابك جيد بواسطة الحصول على تغير ايجابي لمعامل الانكسار كبير مع الحصول على طول ملائم لذراع المفتاح يصل الى 8 مايكرومتر مع قدرة تجهيز واطئة تصل الى  $4\text{ V}/\mu\text{m}$ . كذلك باستخدام مادة الليثيوم تننليات تم انجاز كفاءة افضل للنظام باستخدام الاطوال الموجية تحت الحمراء.

## **1. Introduction**

To plan and improve the waveguide of optical devices it is important to compute characteristics values, that characterized optical overlap (optical confinement factor), thus the reaction of light with the surround material [1]. The overall performance of a modulator depended linearity on the capability for the optical mode to overlap with the effective material (i.e., applied electric field on the material). A contrast of the modulation overall performance as a

function of optical overlap[2]. The optical overlap,  $\Gamma$ , known as the portion of the optical field overlapping with the applied electric field on the material [3] and specifically, it appears how well the guided mode field is limited in a specific locale [1]. Thus, in silicon nitride-lithium niobate Si-LN optical device a small overlap establishes between apportion of the mode power and the lithium niobate LN region because of it supports a distributed optical mode within silicon nitride-lithium niobate Si/LN waveguide thus the

modulation efficiency is low [4]. A large optical overlap achieved in the lithium niobate LN layer on insulator which improved as a better platform to plan waveguides [5-16]. In the electro-optic E-O polymer device the optical overlap depends on dimensions of the cavity and width of electrode such as in dimensions of 240 and 110 nm for width of electrode and cavity respectively, the optical overlap is great, otherwise in the case the width of electrodes and gap

varied by  $\pm 30$  nm, the optical overlap is reduced by 3%, see figure (1) [17]. In the Silicone electro-optic devices, the optical overlap can be increased by fabricating optical devices with thicker hybrid barium titanate BTO, where by the fabricating optical devices support other a singular transverse electric TE-mode where the optical power confined in the layer of the electro-optic active barium titanate BTO by 18% [18].

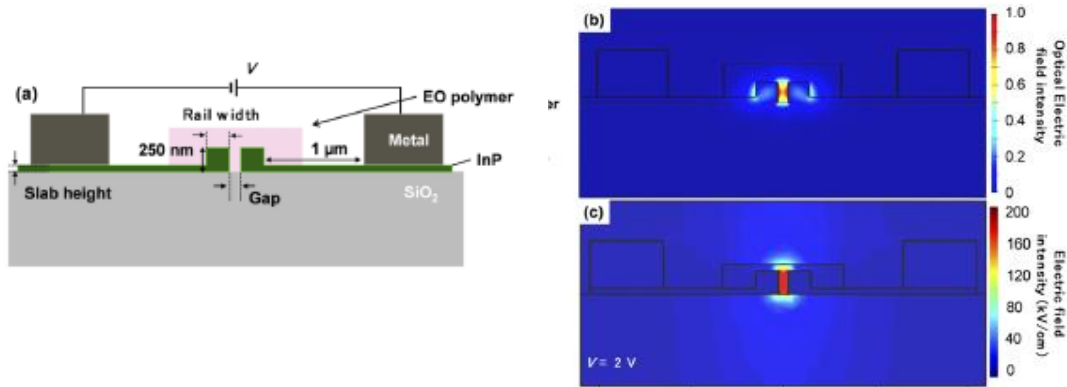


**Figure (1):** (a) Electro-optic polymer with cross section structure, (b) Distribution of optical electric field for slot mod of Inp slot waveguide, (c) Distribution of DC electrical field on waveguide of InP slot [17]

This paper introduces a model to solve a problem of overlap for length of arm with the ordinary positive changing index of refractive by applied of electric field. It utilizes a 2x2 Mach-Zehnder interferometer MZI electro-optic switch depends on electro-optic effect (Pockel effect) for LiTaO<sub>3</sub> as shown in Fig. 2 and Table 1.

equal length arm where the intensity of light it was modulated with phase difference  $\Delta\phi$  and applied electric field  $E$ . Addition a constructive of interference was happened because of the lengths of optical path for arm is same at result to recombined of optical waves on the end of arms switch whereupon:

**Table (1):** electro-optic coefficients ( $r_{33}$ ), refractive index ( $n_o$ ) and wavelengths ( $\lambda$ ), for LiTaO<sub>3</sub>

$R_{33}(Pm/V)$	Ordinary refractive index $n_o$	Wavelength (nm)	Ref.
$30.5 \pm 0.3$	2.1763	632.8	[19]
$27.4 \pm 0.3$	2.1186	1558	[19]

$$I = I_o \cos^2 \left( \frac{\Delta\phi}{2} \right) \quad \dots (1)$$

$$E = E_o e^{i(Kx - \omega t)} \quad \dots (2)$$

$$E = E_o \cos \left( \frac{\Delta\phi}{2} \right) e^{i(Kx - \omega t)} \quad \dots (3)$$

Therefore, when applied electric field a long of optical axis of crystal material the refractive index changes, as shown in Fig. (3) whereupon [20].

$$\Delta n_x = \frac{1}{2} n_x^3 r_{33} E \quad \dots (4)$$

Where  $r_{33}$  is electro-optic coefficient and  $n_x$  is refractive index in the x-direction. In addition, it employs a crystal material and a suitable polarizer as shown in Fig. 3 a phase modulated can be induced without modified in intensity or polarization thus, a drive voltage rotates the main optic axis in the cross section of crystal. The switching voltage is on/off when a polarizer puts in the parallel shape to only one of the main optic axes. Therefore, the input electrical-optical field in direction of x and the output optical wave whereupon [20]:

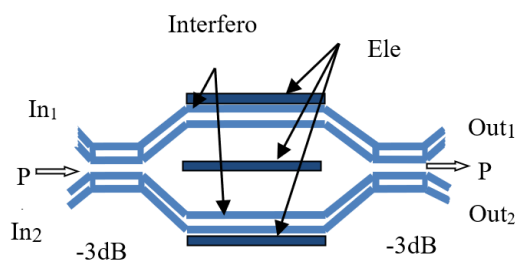


**Figure (2):** 2x2 Mach-Zehnder interferometer MZI electro-optic switch base on the electro-optic impact

In this system A Mach-Zehnder interferometer MZI consists of two branches of interferometer with

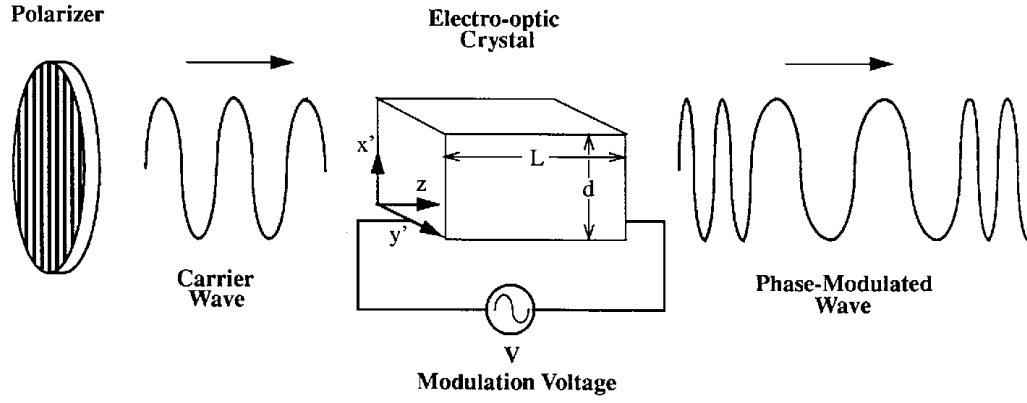


Figure (3): Applied an electrical field on the electro-optic crystal

$$E_i(t) = E_i \cos \omega t \quad \dots (5)$$

$$E_o(t) = E_i \cos(\omega t - \phi) \quad \dots (6)$$

Thus,

$$\phi = \frac{2\pi}{\lambda} (n_x - \Delta n_x)L = \phi_o + \Delta\phi_x \quad \dots (7)$$

The expression of  $\phi$  considered a totality phase shift included the ordinary phase term  $\phi_o$ , L is length of crystal, and  $\Delta\phi_x$  is electrically changing phase as [20].

$$\Delta\phi_x = \frac{2\pi L \Delta n_x}{\lambda} \quad \dots (8)$$

Where the half-wave voltage switching voltage  $V\pi$  is :

$$V\pi = \frac{d\lambda}{Lr_{33}n_o^3} \quad \dots (9)$$

Where d is the waveguide gap in  $\mu m$ .

## 2. Analytical switch

The equation of the optical switch, in which the event light separates in two branches ( $I_{o1}$  and  $I_{o2}$ ), and an optical path will combine on the end of switch as ( $I_2 = I_{o1} + I_{o2}$ ), also,  $I_1$  represents electro-optic output power. in this case:

$$\frac{2I_1}{I_2} = \frac{2E[(E-1) + (1-E)\cos\Delta\phi]}{2E[(E-1) + (1-E)\cos\Delta\phi] + 1} \quad \dots (10)$$

An electro-optic switch will drive by applied an electric field on the arm as known in equation (2).

$$E = \frac{2\Delta n}{r_{33}\Gamma n_o^3} \quad \dots (11)$$

Where electric field  $E = \frac{V}{d}$  in  $V/\mu m$ , and  $\Gamma$  is optical overlap (unit less).

$$Y = \left( \frac{2\Delta n}{r_{33}\Gamma n_o^3} - 1 \right) + \left( 1 - \frac{2\Delta n}{r_{33}\Gamma n_o^3} \right) \cos \Delta\phi$$

$$= \frac{2\Delta n - r_{33}\Gamma n_o^3}{r_{33}\Gamma n_o^3} + \frac{(r_{33}\Gamma n_o^3 - 2\Delta n)}{r_{33}\Gamma n_o^3} \cos \Delta\phi$$

$$\frac{2I_1}{I_2} = \frac{4\Delta n}{r_{33}\Gamma n_o^3} Y + 1$$

$$M = (4\Delta n r_{33}\Gamma n_o^3 - 8\Delta n^2) \cos \Delta\phi$$

$$Z = \frac{8\Delta n^2 + 4\Delta n r_{33}\Gamma n_o^3 + M}{r_{33}^2 \Gamma^2 n_o^6}$$

$$\frac{2I_1}{I_2} = Z + 1$$

$$\frac{2I_1}{I_2} = \frac{r_{33}^2 \Gamma^2 n_o^6 + 8\Delta n^2 + 4\Delta n r_{33}\Gamma n_o^3 + M}{r_{33}^2 \Gamma^2 n_o^6}$$

$$I_2(r_{33}^2 \Gamma^2 n_o^6 + 8\Delta n^2 + 4\Delta n r_{33}\Gamma n_o^3 + M) = 2I_1 r_{33}^2 \Gamma^2 n_o^6$$

$$N = 2I_1 r_{33}^2 \Gamma^2 n_o^6 - I_2 r_{33}^2 \Gamma^2 n_o^6 - 8\Delta n^2 I_2 - 4\Delta n I_2 r_{33}\Gamma n_o^3$$

$$I_2 M = N$$

$$\cos \Delta\phi = \frac{N}{I_2(4\Delta n r_{33}\Gamma n_o^3 - 8\Delta n^2)}$$

$$\cos \Delta\phi = \frac{(2I_1 - I_2)r_{33}^2 \Gamma^2 n_o^6}{I_2(4\Delta n r_{33}\Gamma n_o^3 - 8\Delta n^2)} + 1 \quad \dots (12)$$

$$\cos \Delta\phi - 1 = \frac{(2I_1 - I_2)r_{33}^2 \Gamma^2 n_o^6}{I_2(4\Delta n r_{33}\Gamma n_o^3 - 8\Delta n^2)} \quad \dots (13)$$

$$B = 4I_2 \Delta n r_{33}\Gamma n_o^3 \cos \Delta\phi - 4I_2 \Delta n r_{33}\Gamma n_o^3 - 8\Delta n^2 \cos \Delta\phi + 8\Delta n^2$$

$$B = (2I_1 - I_2)r_{33}^2 \Gamma^2 n_o^6$$

$$F = \Delta n(4I_2 r_{33}\Gamma n_o^3 \cos \Delta\phi - 4I_2 r_{33}\Gamma n_o^3) + r_{33}^2 \Gamma^2 n_o^6(I_2 - 2I_1)$$

$$\Delta n^2(8 - 8 \cos \Delta\phi) + F = 0$$

$$\therefore \Delta\phi = \frac{\pi L n_o^3 r_{33} V}{\lambda d} \quad \dots (14)$$

$$\Delta n = \frac{-(4I_2 r_{33}\Gamma n_o^3 \cos \Delta\phi - 4I_2 r_{33}\Gamma n_o^3) \pm J}{16(1 - \cos \Delta\phi)} \quad \dots (15)$$

$$J = \sqrt{(4I_2 r_{33}\Gamma n_o^3 \cos \Delta\phi - 4I_2 r_{33}\Gamma n_o^3)^2 - 4(I_2 - 2I_1)r_{33}^2 \Gamma^2 n_o^6(8 - 8 \cos \Delta\phi)}$$

## 3. Results and discussions:

This study suggests a model for propose a type of optical device a 2x2 Mach-Zehnder interferometer electro-optical switch base on lithium tantalite  $LiTaO_3$  when an overlap is important factor for enhancement the performance of electro-optic switch. Also, the electro-optic effect (Pockel effect) is useful, where the performance of switch will evaluate using the equation.15. In this paper, the type of device configuration is transverse where the voltage applied perpendicular to the direction of propagation, thus, the gap between electrodes d acts as capacitor in



which  $d$  restricts the speed of MZI electro-optic switch (i.e., the speed of switching), addition, the electric field because  $E = V/d$ , therefore, the reduction of  $d$  creates the electric field  $E$  increases, thus, the ordinary positive refractive index changes  $\Delta n$  will rise, also, the  $\Delta n$  will inversely proportional to the gap between electrodes  $d$  as equation(11), therefore, the reduction of  $d$  results to large overlap because of the  $\Delta n$  is large, also, in the case transvers configuration the aspect ratio  $L/d$  is very large because of the electrodes not restricted the passing of optical light through arms of switch, thus the aspect ratio effective factor to be induced phase shift because the large aspect ratio due to small induced phase shift and vice versa, then, it will result the high quality switching, better modulation, and large overlap. Also, in the case it applies electric field about  $4V/\mu m$ , the ordinary positive refractive index changes and considers very low power consumption, thus, the better performance for switch achieves also, the overlap is large which depends on the gap between electrodes  $d$ , length of arms  $L$ , and the ordinary positive refractive index change  $\Delta n$ , so it must be choose an appropriate length for arm that relative to a large applied of electric field, with the small  $d$  therefore, when the arm about  $8\mu m$  with larger ordinary positive changing of refractive index  $\Delta n$ , the overlap is better, as shown in Figs. 4 and 5. In addition, the small refractive index  $n_o$  and electro-optic coefficient  $r_{33}$  leads to large overlap, therefore, these factors are inversely proportional to the overlap  $\Gamma$  as equation(11), thus. the positive changing of refractive index and length of arm are large these, result a better overlap by limited the  $n_o$  and  $r_{33}$ , as shown in Figs. 6 & 7. Also, the operating wavelengths improve the performance of electro-optic switch with applying electric field because, it uses wide band of wavelength thus, the ordinary positive changing of refractive index is better, as shown in Fig. 8.

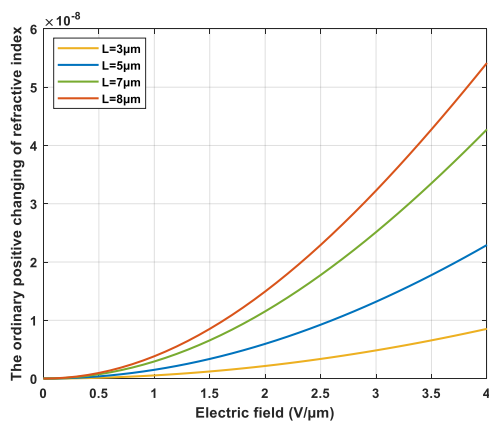


**Figure (4):** The ordinary positive changing of refractive index by applying electrical field with different length of arms

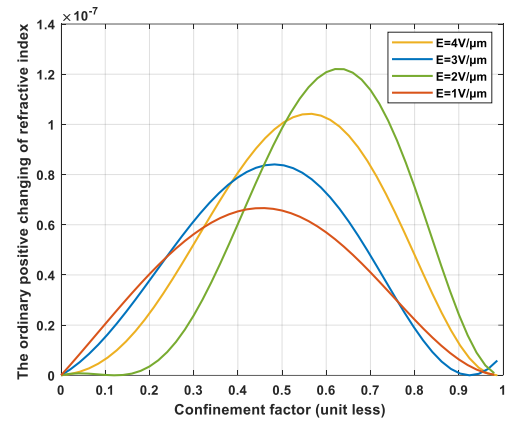


**Figure (5):** The ordinary positive changing of refractive index as a function of confinement factor with different applying electrical field

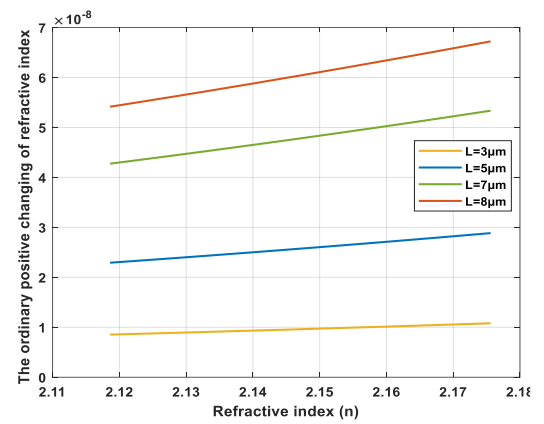


**Figure (6):** The ordinary positive changing of refractive index as a function of refractive index with different length of arms for  $LiTaO_3$

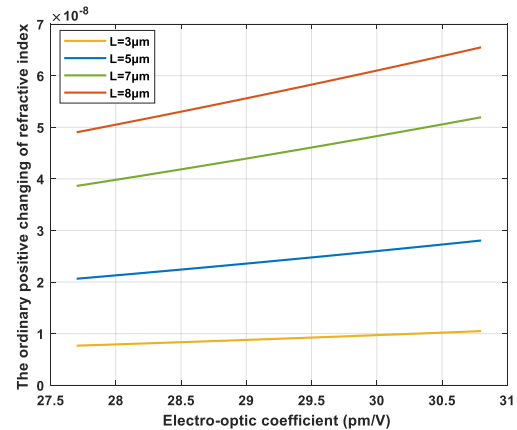


**Figure (7):** The ordinary positive changing of electro-optic coefficient as a function of electro-optic coefficient with different length of arms for  $LiTaO_3$

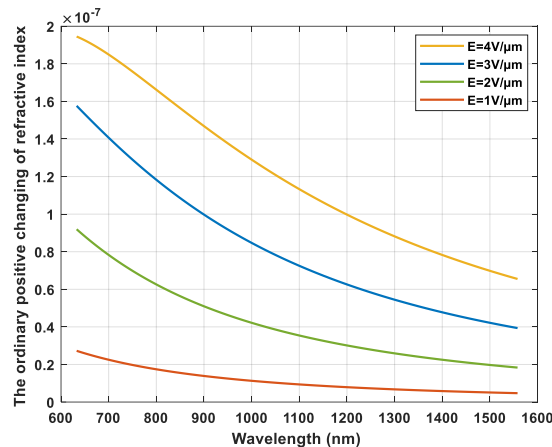


**Figure (8):** The ordinary positive changing of refractive index with wavelength and different applying electrical field for LiTaO<sub>3</sub>

#### 4. Conclusions

This study proposes model for enhancement of a 2×2 Mach-Zehnder interferometer optical switch for lithium tantalite LiTaO<sub>3</sub>, which base on electro-optic effect (Pockels effect). This research improves the performance of switch by reduction of gap between the electrodes d, thus it achieves a high quality overlap, and this is by a large positive changing of refractive index with better small length about 8μm, and low driving power electric field at least 4V/μm. In addition, for lithium tantalite LiTaO<sub>3</sub>, it uses a wide band of wavelengths therefore, it improves the performance of electro-optic switch.

#### 5. References:

- [1] P. S., "Silicon-On-Insulator Slot Waveguides: Theory and Optics and Optical Sensing," Technical University of Applied Sciences Wildau, Germany, 2018.
- [2] Z. Ma, M. H. Tahersima, S. Khan, V. J. Sorger., "Two-Dimensional Material-Based Mode Confinement Engineering in Electro-Optic Modulators," IEEE Journal of Selected Topics in Quantum Electronics, vol. 23, no. 1, 1-8 .2017.
- [3] Z. Ma, R. Hemnani, L. Bartels, R. Agarwa, V, J. Sorger., "2D Materials in Electro-Optic Modulation: energy efficiency, electrostatics, mode overlap, material transfer and integration," Appl. Phys, 2018.
- [4] M. He, M. Xu, Y. Ren, J. Jian, Z. Ruan, Y. Xu, S. Gao, S. Sun, X. Wen, L. Zhou, L. Liu, C. Guo, H. Chen, S. Yu, and X. Cai., " High-Performance Hybrid Silicon and Lithium Niobate Mach-Zehnder Modulators for 100 Gbit/s and Beyond," Nature photonic, 2019.
- [5] R., G. et al., "Single Carrier High Symbol Rate Transmitter for Data Rates up to 1.0 Tb/s," In Optical Fiber Communication Conference.Th3A.2, OSA, Anaheim, 2016.
- [6] J., D., Tulli, D., G., M., B., M. & P., V., "Micro-structured integrated electro-optic LiNbO<sub>3</sub>modulators," Laser Photon. Rev.3, 301-313, 2009.
- [7] P,j, G., Hu, H., S., W. & Günter, P., "Lithium niobate on insulator (LNOI) for micro-phonic devices, " Laser Photon. Rev.6, 488-503, 2012.
- [8] G., A., P., G., R., D., D., R. & Günter, P., "Electro-optically tunable microring resonators in lithium niobate, " Nat. Photon.1, 407, 2007.
- [9] J., S., Xu, L., Zhang, H. & Li, Y. "LiNbO<sub>3</sub> thin-film modulators using silicon nitride surface ridge waveguides". IEEE Photon. Technol. Lett. 28, 736-739, 2016.
- [10] R., A. et al., "High-performance and linear thin-film lithium niobate Mach-Zehnder modulators on silicon up to 50 GHz, " Opt. Lett. 41, 5700-5703, 2016.
- [11] W., J. et al., "High-Q lithium niobate microdisk resonators on a chip for efficient electro-optic modulation," Opt. Exp. 23, 23072-23078, 2015.
- [12] C., L., K., Y. & Hu, H., "Electric-optical property of the proton exchanged phase modulator in single-crystal lithium niobate thin film, "Opt. Exp. 24, 4640-4647, 2016.
- [13] C., L. et al., "Thin film wavelength converters for photonic integrated circuits, " Optica 3, 531-535, 2016.
- [14] C., L. et al., "Heterogeneous integration of lithium niobate and silicon nitride waveguides for wafer-scale photonic integrated circuits on silicon, " Opt. Lett.42, 803-806. 2017.
- [15] W., C. et al., "Integrated lithium niobate electro-optic modulators operating at CMOS-compatible voltages, "Nature562, 101-104, 2018.
- [16] B., A., Corcoran, B., Chang, L., Bowers, J. & Mitchell, A., "Status and Potential of Lithium Niobate on Insulator (LNOI) for Photonic Integrated Circuits, "Laser Photon. Rev. 12, 1700256. 2018.
- [17] N. Sekine, K. Toprasertpong, S. Takagi, and M. Takenaka., "Numerical analyses of optical loss and modulation bandwidth of an InP organic hybrid optical modulator, "Optics express, 2020.
- [18] J. E. Ortmann, F. Eltes, D. Caimi, N. Meier, I. A. Demkov, L. Czornomaz, J. Fompeyrine, and S. Abel., "Ultra-Low-Power Tuning in Hybrid Barium Titanate-Silicon Nitride Electro-Optic Devices on Silicon," Photonics, 2019.
- [19] J. L. Casson et al., "Electro-optic coefficients of lithium tantalate at near-infrared wavelengths," JOSA B, vol. 21, no. 11, pp. 1948-1952, 2004.
- [20] T. A. Maldonado., "Electro-optic modulator," chapter13, department of electrical engineering. The University of Texas at Arlington.